

ENHANCING COVID-19 SEVERITY ANALYSIS THROUGH ENSEMBLE METHODS

Anand Thyagachandran, Hema A Murthy

Department of Computer Science and Engineering,
Indian Institute of Technology Madras, India
{tanand, hema}@cse.iitm.ac.in

ABSTRACT

Computed Tomography (CT) scans provide a detailed image of the lungs, allowing clinicians to observe the extent of damage caused by COVID-19. The CT severity score (CTSS) of COVID-19 can be categorized based on the extent of lung involvement observed on a CT scan. This paper proposes a domain knowledge-based pipeline to extract the infection regions using diverse image-processing algorithms and a pre-trained UNET model. An ensemble of three machine-learning models, Random Forest (RF), Extremely Randomized Trees (ERT), and Support Vector Machine (SVM), is employed to classify the CT scans into different severity classes. The proposed system achieved a macro F1 score of 58% on the validation dataset in the AI-Enabled Medical Image Analysis Workshop and COVID-19 Diagnosis Competition (AI-MIA-COV19D).

Index Terms— COVID-19, CT-Scans, Infection Segmentation, Machine Learning Methods, Severity Analysis

1. INTRODUCTION

The outbreak of COVID-19 has resulted in a substantial need for prompt and precise diagnostic testing to detect individuals who may have contracted the SARS-CoV-2 virus. Laboratory tests such as Reverse Transcription Polymerase Chain Reaction (RT-PCR) [1] and antigen tests are commonly used for diagnosing COVID-19. While these tests detect the virus's presence from the respiratory samples [2], but fail to provide an accurate analysis of the disease severity. Additional diagnostic tools are needed to assess the extent of lung damage. Radiological imaging of the chest, including chest radiography and CT scans, is essential to assess the severity of COVID-19 infections [3]. While chest X-rays do not furnish sufficient resolution to evaluate the extent of lung damage. CT scans provide a more detailed view of the lungs and can identify the distribution and extent of infection. Clinicians can comprehend critical information to gauge the severity of the disease and deliver timely and effective treatment to the patients.

Radiologists typically observe ground-glass opacities (GGO) [4], which indicate lung inflammation but that do

Table 1. Summary of the dataset (COVID-19-CT-DB)

Category	Train	Validation
Mild	133	31
Moderate	124	20
Severe	166	45
Critical	39	5

not obstruct the underlying pulmonary vessels. Consolidations are the advanced stage of GGO and hide the underlying vessels [5]. Pleural effusion occurs when fluid accumulates excessively in the pleural space surrounding the lungs and is a highly severe case of COVID-19 [6]. These clinical features are critical in identifying and diagnosing COVID-19 in patients [7]. In addition to GGO and consolidations, radiologists observe features such as the halo sign (central consolidations surrounded by GGO), the reverse halo sign (central ground-glass lucent area with peripheral consolidation), and crazy paving patterns. These features and their distribution provide crucial information to diagnose and manage COVID-19 patients [4, 8].

Machine learning and deep learning methods have been extensively encountered to classify CT scans and infection segmentation. The classification task between COVID-19 and non-COVID-19 is proposed in various studies such as [9, 10, 11, 12]. Additionally, some studies have extended the classification task to include three categories - COVID-19, Community-acquired Pneumonia (CAP), and Normal, such as [13, 14, 15, 16]. COVID-19 and CAP diseases share similar features; distinguishing between these two categories is crucial to monitor the progression of COVID-19, which tends to be much faster than that of CAP. These methods fail to identify the severity of patients. Further, many research works have been focused on the infection region segmentation from CT scans that can be used for severity analysis. Generating large medical image datasets for infection segmentation is time-consuming and requires highly qualified domain experts to annotate the data. Different strategies are proposed to address the unavailability of the large corpus, such as semi-supervised method (small dataset is used for

Table 2. Different classes of severity and its characteristics in the given dataset [29].

Category	Severity	Description
1	Mild	Few or no GGOs. Pulmonary parenchymal involvement $\leq 25\%$ or absence
2	Moderate	Ground glass opacities. Pulmonary parenchymal involvement $25 \leq 50\%$
3	Severe	Ground glass opacities. Pulmonary parenchymal involvement $50 \leq 75\%$
4	Critical	Ground glass opacities. Pulmonary parenchymal involvement $\geq 75\%$

supervised training along with a large amount of unlabelled data) [17, 18], weakly supervised way (ground truth data used partially in training process) [19, 20], and unsupervised methods (without any ground truth data) [21, 22]. A criterion on the volume of infection has been used as an indicator of the severity of infection [23, 24] and classified the CT scans into different classes such as healthy, mild, moderate, severe, and critical.

Radiologists commonly use the CT severity score (CTSS) to determine the extent of severity in COVID-19 patients [25]. The score ranges from 0 to 25 and is calculated based on the distribution and magnitude of abnormalities seen on chest CT scans. A higher CTSS score indicates more severe lung damage, and this information is essential in making appropriate treatment decisions [26, 27]. In line with this approach, we have developed an automatic method that categorizes CT severity into four classes: mild, moderate, severe, and critical. The proposed method employs various image processing algorithms, and a pre-trained U-NET model [28] to extract infected regions from CT scans. Infection rate-based features are generated and are learned by machine learning algorithms to predict the severity classes. A fully automatic severity analysis model can significantly reduce clinicians’ time to assess a patient’s condition.

The paper is organized as follows: **Section 2** explains the dataset used in the study. **Section 3** presents the proposed method for segmenting relevant clinical features and classifying COVID-19 patients into different severity classes. **Section 4** discusses results and inferences. Finally, **Section 5** summarizes the present study.

2. DATASET

The COVID-19-CT-Database (COVID-19-CT-DB) is provided as part of the "AI-enabled Medical Image Analysis Workshop, and COVID-19 Diagnosis Competition (AI-MIA-COV19D)" [30, 31, 32, 33, 34, 35]. The CT scans were collected from September 1, 2020, to March 31, 2021. Four highly experienced medical experts annotated these CT scans (two radiologists and two pulmonologists).

Generally, CT scans are volumetric data (3D scans) and

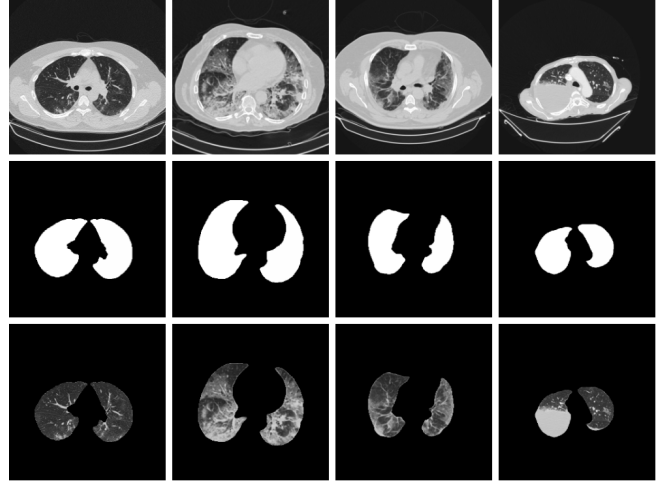


Fig. 1. First row represents CT scan images of mild, moderate, severe, and critical categories provided in the challenge. The second row shows the lung mask generated from the images. The third row depicts the segmented region of interest for further analysis of each category.

are available mainly in Digital Imaging and Communications in Medicine (DICOM) and Neuroimaging Informatics Technology Initiative (NIfTI) formats. These two image formats represent the CT scan image in higher resolution, also known as Hounsfield Units (HU). Radiologists use a mapping table to identify the different parts of the CT scan images based on the HU values. The COVID-19-CT-DB dataset is converted from the HU scale image into an 8-bit gray-scale (JPG) image. This down-sampling process introduces an information loss and reduction in the resolution of the CT scan images. The summary of the severity analysis dataset is shown in **Table 1**, and the description of severity categories is given in **Table 2**.

3. PROPOSED METHOD

The proposed pipeline consists of two parts, lesion segmentation from the CT scan and quantifying the severity of the infection rate. The proposed method uses various image processing algorithms, machine learning, and deep learning models to predict the severity of the COVID-19 patient.

3.1. Infection Segmentation

The infection segmentation pipeline uses domain knowledge to extract the infection regions. Initially, a pre-trained UNET model extracts the lung region from the image. Then, the image’s contrast is enhanced by histogram hyperbolization [36]. Next, top-hat morphological operations are applied to remove blood vessels from the image [37]. Finally, the resultant image combines various morphological operations to fine-tune

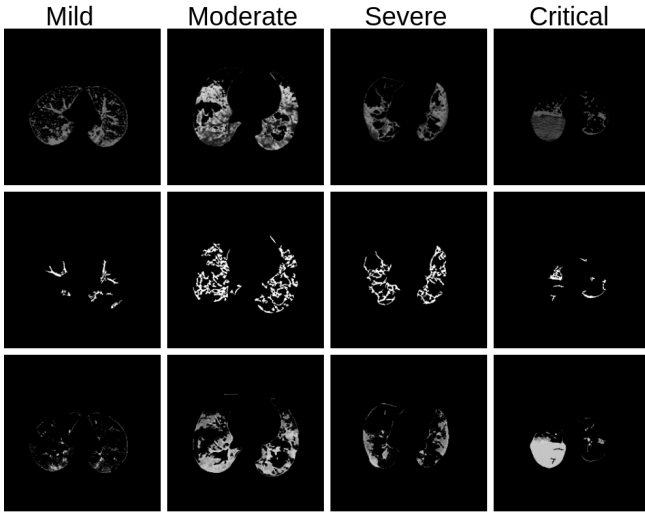


Fig. 2. First row shows the histogram hyperbolized lung region of mild, moderate, severe, and critical classes. The second row depicts enhanced blood vessels using top-hat transform. The third row represents the extracted infection regions.

the infection regions.

3.1.1. Lung Mask Generation

This module aims to extract the lung region from the lung CT scan. The chest CT scan contains the lung region and organs like the trachea, diaphragm, heart, stomach, and tissues. This module uses a convolutional neural network model to generate a mask to retain the region of interest from the lung CT scan. A pre-trained UNET [28] architecture is used to extract the lung region from the CT scan images. This model is trained on the HU scale CT images, and the given dataset contains images in JPG format. The input CT scans are converted to HU scale images using a linear transformation.

The UNET model is an end-to-end fully convolution neural network comprising a contraction and expansion path. The contracting path consists of 2D convolution layers, a nonlinear activation function, and average pooling layers. A high-dimensional feature map is finally generated. This feature map is up-sampled (by using transposed convolution) and concatenated with the feature map generated from the contracting path through skip connections. These concatenated feature maps are passed through 2D convolution layers and nonlinear activation functions in the expanding path to produce a segmentation mask from the feature map. This is primarily an encoder-decoder model.

The lung mask involvement accounts for variations in the number of CT image slices across patients. An empirical threshold on the lung mask's involvement and a threshold on the number of slices from the middle region (slice number which lies between one-third to two-thirds of the total num-

ber of slices) are used to select the CT scan images for further analysis. The CT scan image is segmented and is applied with a Gaussian filter to smooth the image without significantly reducing the sharpness of the edges. Further, this image is fed to the image enhancement module. The lung masks and segmented regions of interest in different categories of COVID-19 severity are shown in **Fig. 1**.

3.1.2. Image Enhancement using Histogram Hyperbolization

Histogram hyperbolization, introduced in [36], is a non-linear image enhancement method that improves the contrast of an image by adjusting its perceived brightness levels. The goal of histogram hyperbolization is to create a function that equalizes the probability of all the perceived brightness levels in the image.

$$J(I) = c(\exp[\log(1 + \frac{1}{c}) * \text{normcm}[I]] - 1) \quad (1)$$

where $J(I)$ is the space-invariant hyperbolization transformation of the image I . c is an empirical threshold. normcm is the normalized cumulative distribution of the intensity histogram. The contrast-enhanced image contains infection regions and the pulmonary vessels. The contrast-enhanced lung region of the CT scan images using histogram hyperbolization is shown in **Fig. 2**.

Algorithm 1: The proposed algorithm to extract the infection regions from CT scans

```

Input: CT Scan (3D Data) – V
Output: Stacked infection regions from CT scans – S
1 for Image in V do
2   Lung_mask  $\leftarrow$  UNET(HU_Image(Image))
3   Seg_img  $\leftarrow$  Lung_mask * Image
4   if (Sum(Lung_mask)  $\geq$  10000 and Position(Image)  $\geq$ 
      Len(V)/3 and Position(Image)  $\leq$  Len(V) * 2/3) or
      (Sum(Lung_mask)  $\geq$  (0.7 * (512 * 512))) then
5     Mask1  $\leftarrow$  Threshold_intensity_filter(Seg_img)
6     Seg_img  $\leftarrow$  Mask1 * Seg_img
7     CT_hyper  $\leftarrow$ 
      Hyperbolization(Gaussian_filter(Seg_img))
8     CT_hyper_new  $\leftarrow$ 
      CC_area_filter(MO.open(CT_hyper))
9     Vessel_mask  $\leftarrow$ 
      CC_area_filter(Bin.OTSU(Top_hat(CT_hyper)))
10    temp_mask  $\leftarrow$  CT_hyper_new - Vessel_mask
11    Infection_mask  $\leftarrow$ 
      MO.dilate(Fill_holes(temp_mask))
12    S  $\leftarrow$  Infection_mask
13  else
14    Remove the 2D image from further analysis
15  /* CC:- Connected Component, MO:-
     Morphological operation */
```

3.1.3. Morphological operations

The present work mainly uses three commonly-used morphological operations: dilation, opening, and top-hat [38]. A

Table 3. The results of severity analysis of linear and non-linear classifiers using CT scans.

Models	WAM	LR	NN	Gboost	Adaboost	k-NN	NB	DT	RF	ERT	SVM	Ensemble
Precision	0.38	0.37	0.42	0.61	0.48	0.67	0.56	0.52	0.64	0.68	0.77	0.70
Recall	0.49	0.42	0.43	0.43	0.52	0.51	0.62	0.56	0.50	0.54	0.56	0.54
F1 score	0.40	0.38	0.41	0.45	0.56	0.50	0.52	0.53	0.53	0.58	0.60	0.58

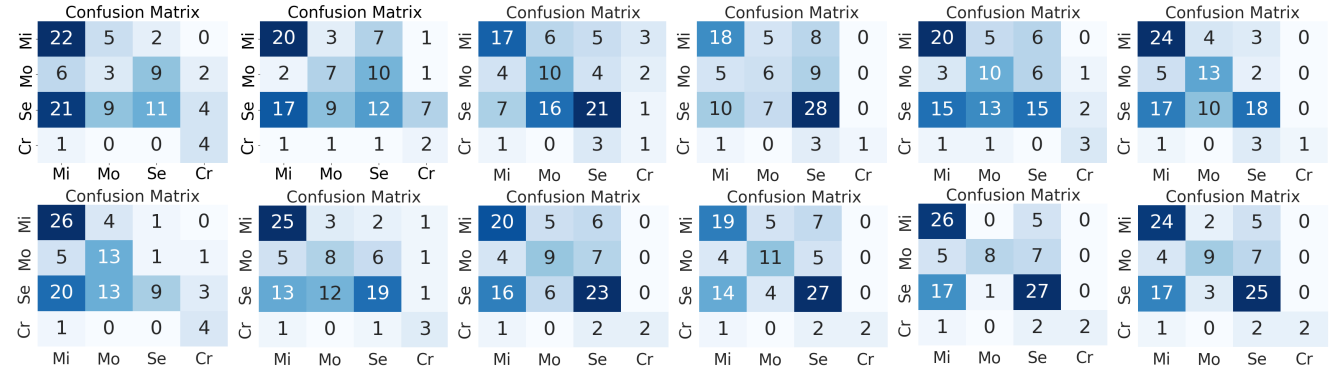


Fig. 3. The first row (from left to right) depicts the confusion matrices of the WAM, LR, NN, Gboost, Adaboost, and k-NN. The second row represents the NB, DT, RF, ERT, SVM, and ensemble classifiers. The axis labels such as Mi-mild, Mo-moderate, Se-severe, and Cr-critical.

kernel matrix (a rectangular kernel (3 x 3)) is used to convolve with the input image. The dilation operation chooses the maximum pixel value from each (3 x 3) neighborhood and replaces the center pixel. The erosion operation finds the minimum pixel value from the kernel neighborhood. The open morphological procedure removes any small foreground objects from the binary image by employing the erosion operation followed by the dilation operation. The top-hat transformation enhances blood vessel-like structures by subtracting the image from its open morphological image. An area-based foreground filter is used to enhance smaller connected objects.

The OTSU adaptive binarization method [39] is applied to the contrast-enhanced image from the previous module. Morphological operation top-hat transform is used to enhance and remove the blood vessels. The resultant image is then fed to morphological operations open and area-based foreground filter to remove the small connected components in the resultant image. The dilation operation is used to fine-tune the boundary of the extracted infection region. The enhanced blood vessels and infection masks generated from the different severity classes are shown in **Fig. 2**.

3.2. Lesion To Severity Score

This section describes the various methods explored to identify the correlation between the infection regions in the CT images and their severity class. Inspired by the CTSS method, a weighted average on the percentage of infection in the left

and right lungs is estimated. Further, various machine learning algorithms are experimented with to classify the CT scan into different severity classes.

3.2.1. Weighted Average Method (WAM)

The infection rate in the left and right lungs is estimated with the infection mask and the UNET lung mask for each slice in the CT scan. A score ranging from one to four is assigned based on the percentage of infection, one (5 - 25% percentage), two (25 - 50% percentage), three (50 - 75% percentage), and four (75 - 100 % percentage). In CTSS estimation, the right lung is divided into three lobes and the left into two lobes, and each lobe's degree of involvement is visually determined. The lobe scores are calculated by the percentage of infection involvement in lobes [40]. An average score across lobes and sum up it into the final CTSS. In the WAM, we employed a similar approach, a proportional weighted average method, to find the severity score for each CT scan slice. Specifically, the right lung region is multiplied by a weight of three and the left lung region by two. The severity score is estimated by averaging the scores across the CT scan images.

3.2.2. Non-linear Methods

This study utilizes a feature vector with a dimension to represent a CT scan. Two features are extracted from each image, such as the left and right lung infection rates. Two methods are employed for a fixed-length representation of the CT scans. If the CT scan contains more than 40 slices, the slices

are uniformly divided into forty regions, choosing the median slice features from each region. On the other hand, the feature vector is enhanced by computing the average percentage of infection from the available slices and appending it to generate an 80-dimensional vector. Machine learning models, including logistic regression (LR), shallow neural network (NN), gradient boost (Gboost), Ada boost, k-nearest neighbor (k-NN), naive Bayes (NB), decision tree (DT), random forest (RF), extremely randomized tree (ERT) [41], support vector machine (SVM), and ensemble models, are employed to learn from these feature representations to predict the severity classes. The machine learning models are implemented with the help of the `sklearn` library in Python. The training data consists of inconsistencies in the dimension of the CT scan images. The images with dimensions (512 x 512) are used to generate the 80-dimensional feature vectors.

4. RESULTS AND DISCUSSIONS

The proposed pipeline aims to identify the correlation between the severity class and the lung infection rate. The weighted average method finds a linear mapping between the infection rate and the severity classes, which yielded a macro F1 score of 0.40. This result led to the realization of the non-linear relationship between the infection rate and severity analysis, prompting the exploration of various machine-learning methods. The results of various classifiers are shown in **Fig. 3** and tabulated in **Table 3**.

The machine learning models achieve better results (regarding macro F1 score) than the WAM except for logistic regression. The RF, ERT, and SVM serve top-3 performing models for the severity analysis. An ensemble of these models achieves the second-best-performing system in the experiments. The ensemble model can improve the accuracy and robustness of predictions, reduce over-fitting, and improve the model's generalization. The confusion matrices show that the mild class achieves higher classification accuracy and less misclassification with other classes. In the case of the moderate class, the trained models are confused with the severe classes; the SVM, Ensemble, and DT models provide more misclassifications to the severe category compared to the mild category. Similarly, the severe class CT scans are misclassified mostly to the mild class. This is due to the inability of the pre-trained UNET model to extract the infection regions connected to the lung boundary. If the infection is distributed to the peripheral areas, then the UNET model cannot distinguish between the lung boundary and the infection regions, which leads to erroneous lung mask generation.

The standard evaluation metrics, such as precision, recall, and macro F1 score, are used to evaluate the models. The performance of linear and non-linear classifiers is shown in **Table 3**. The baseline model is based on a convolutional neural network (CNN)- recurrent neural network (RNN) where the CNN is used as a feature extractor and RNN is used to model

the sequence of features extracted from the CT scan images. It is observed that all non-linear models, except logistic regression, outperformed the baseline model. An ensemble of RF, ERT, and SVM models achieves the best result for the validation data.

5. CONCLUSION

In this paper, we proposed a domain knowledge-based preprocessing pipeline to extract the relevant lesion regions. Infection rate-based features are proposed. Linear and non-linear models are used to predict the CT scan severity class. The ensemble model of the random forest, extremely randomized tree, and SVM achieves a macro F1 score of 58%.

6. REFERENCES

- [1] Shannon L Emery et al., “Real-time reverse transcription–polymerase chain reaction assay for sars-associated coronavirus,” *Emerging infectious diseases*, vol. 10, no. 2, pp. 311, 2004.
- [2] Moustapha Dramé et al., “Should rt-pcr be considered a gold standard in the diagnosis of covid-19?,” *Journal of medical virology*, 2020.
- [3] Elmehdi Benmalek et al., “Comparing ct scan and chest x-ray imaging for covid-19 diagnosis,” *Biomedical Engineering Advances*, vol. 1, pp. 100003, 2021.
- [4] Thomas C Kwee and Robert M Kwee, “Chest ct in covid-19: what the radiologist needs to know,” *Radiographics*, vol. 40, no. 7, pp. 1848–1865, 2020.
- [5] Minhua Yu et al., “Thin-section chest ct imaging of covid-19 pneumonia: a comparison between patients with mild and severe disease,” *Radiology: Cardiothoracic Imaging*, vol. 2, no. 2, pp. e200126, 2020.
- [6] Atsushi Nambu et al., “Imaging of community-acquired pneumonia: roles of imaging examinations, imaging diagnosis of specific pathogens and discrimination from noninfectious diseases,” *World Journal of Radiology*, vol. 6, no. 10, pp. 779, 2014.
- [7] Nan Zhang et al., “Clinical characteristics and chest ct imaging features of critically ill covid-19 patients,” *European Radiology*, vol. 30, pp. 6151–6160, 2020.
- [8] Liaoyi Lin et al., “Ct manifestations of coronavirus disease (covid-19) pneumonia and influenza virus pneumonia: A comparative study,” *American Journal of Roentgenology*, vol. 216, no. 1, pp. 71–79, 2021.
- [9] Junlin Hou et al., “Cmc-cov19d: Contrastive mixup classification for covid-19 diagnosis,” in *Proceedings of*

the IEEE/CVF International Conference on Computer Vision (ICCV) Workshops, October 2021, pp. 454–461.

[10] Dimitrios Kollias et al., “Mia-cov19d: Covid-19 detection through 3-d chest ct image analysis,” in *Proceedings of the IEEE/CVF International Conference on Computer Vision (ICCV) Workshops*, October 2021, pp. 537–544.

[11] Shuang Liang et al., “A hybrid and fast deep learning framework for covid-19 detection via 3d chest ct images,” in *Proceedings of the IEEE/CVF International Conference on Computer Vision (ICCV) Workshops*, October 2021, pp. 508–512.

[12] Radu Miron et al., “Evaluating volumetric and slice-based approaches for covid-19 detection in chest cts,” in *Proceedings of the IEEE/CVF International Conference on Computer Vision (ICCV) Workshops*, October 2021, pp. 529–536.

[13] Parnian Afshar et al., “Covid-ct-md, covid-19 computed tomography scan dataset applicable in machine learning and deep learning,” *Scientific Data*, vol. 8, no. 1, pp. 1–8, 2021.

[14] Pratyush Garg et al., “Multi-scale residual network for covid-19 diagnosis using ct-scans,” in *ICASSP 2021-2021 IEEE International Conference on Acoustics, Speech and Signal Processing (ICASSP)*. IEEE, 2021, pp. 8558–8562.

[15] Shubham Chaudhary et al., “Detecting covid-19 and community acquired pneumonia using chest ct scan images with deep learning,” in *ICASSP 2021-2021 IEEE International Conference on Acoustics, Speech and Signal Processing (ICASSP)*. IEEE, 2021, pp. 8583–8587.

[16] Shuohan Xue and Charith Abhayaratne, “Covid-19 diagnostic using 3d deep transfer learning for classification of volumetric computerised tomography chest scans,” in *ICASSP 2021-2021 IEEE International Conference on Acoustics, Speech and Signal Processing (ICASSP)*. IEEE, 2021, pp. 8573–8577.

[17] Deng-Ping Fan et al., “Inf-net: Automatic covid-19 lung infection segmentation from ct images,” *IEEE Transactions on Medical Imaging*, vol. 39, no. 8, pp. 2626–2637, 2020.

[18] Jun Ma et al., “Active contour regularized semi-supervised learning for covid-19 ct infection segmentation with limited annotations,” *Physics in Medicine & Biology*, vol. 65, no. 22, pp. 225034, 2020.

[19] Xinggang Wang et al., “A weakly-supervised framework for covid-19 classification and lesion localization from chest ct,” *IEEE Transactions on Medical Imaging*, vol. 39, no. 8, pp. 2615–2625, 2020.

[20] Zhongyi Han et al., “Accurate screening of covid-19 using attention-based deep 3d multiple instance learning,” *IEEE Transactions on Medical Imaging*, vol. 39, no. 8, pp. 2584–2594, 2020.

[21] Rui Xu et al., “Unsupervised detection of pulmonary opacities for computer-aided diagnosis of covid-19 on ct images,” in *2020 25th International Conference on Pattern Recognition (ICPR)*, 2021, pp. 9007–9014.

[22] Han Chen et al., “Unsupervised domain adaptation based covid-19 ct infection segmentation network,” *Applied Intelligence*, pp. 1–14, 2022.

[23] Ben Ye et al., “Severity assessment of covid-19 based on feature extraction and v-descriptors,” *IEEE Transactions on Industrial Informatics*, vol. 17, no. 11, pp. 7456–7467, 2021.

[24] Yazan Qiblawey et al., “Detection and severity classification of covid-19 in ct images using deep learning,” *Diagnostics*, vol. 11, no. 5, pp. 893, 2021.

[25] Arthur WE Lieveld et al., “Chest ct in covid-19 at the ed: validation of the covid-19 reporting and data system (corrads) and ct severity score: a prospective, multicenter, observational study,” *Chest*, vol. 159, no. 3, pp. 1126–1135, 2021.

[26] Kunwei Li et al., “Ct image visual quantitative evaluation and clinical classification of coronavirus disease (covid-19),” *European radiology*, vol. 30, pp. 4407–4416, 2020.

[27] Kunhua Li et al., “The clinical and chest ct features associated with severe and critical covid-19 pneumonia,” *Investigative radiology*, 2020.

[28] Johannes Hofmanninger et al., “Automatic lung segmentation in routine imaging is primarily a data diversity problem, not a methodology problem,” *European Radiology Experimental*, vol. 4, no. 1, pp. 1–13, 2020.

[29] Dimitrios Kollias, Anastasios Arsenos, and Stefanos Kollias, “Ai-mia: Covid-19 detection and severity analysis through medical imaging,” in *Computer Vision–ECCV 2022 Workshops: Tel Aviv, Israel, October 23–27, 2022, Proceedings, Part VII*. Springer, 2023, pp. 677–690.

[30] Dimitrios Kollias et al., “Ai-mia: Covid-19 detection & severity analysis through medical imaging,” *arXiv preprint arXiv:2206.04732*, 2022.

[31] Anastasios Arsenos et al., “A large imaging database and novel deep neural architecture for covid-19 diagnosis,” in *2022 IEEE 14th Image, Video, and Multidimensional Signal Processing Workshop (IVMSP)*. IEEE, 2022, p. 1–5.

- [32] Dimitrios Kollias et al., “Mia-cov19d: Covid-19 detection through 3-d chest ct image analysis,” in *Proceedings of the IEEE/CVF International Conference on Computer Vision*, 2021, p. 537–544.
- [33] Dimitrios Kollias et al., “Deep transparent prediction through latent representation analysis,” *arXiv preprint arXiv:2009.07044*, 2020.
- [34] Dimitris Kollias et al., “Transparent adaptation in deep medical image diagnosis.,” in *TAILOR*, 2020, p. 251–267.
- [35] Dimitrios Kollias et al., “Deep neural architectures for prediction in healthcare,” *Complex & Intelligent Systems*, vol. 4, no. 2, pp. 119–131, 2018.
- [36] Werner Frei, “Image enhancement by histogram hyperbolization,” *Computer Graphics and Image Processing*, vol. 6, no. 3, pp. 286–294, 1977.
- [37] Yanjie Zhu et al., “Automatic segmentation of ground-glass opacities in lung ct images by using markov random field-based algorithms,” *Journal of digital imaging*, vol. 25, no. 3, pp. 409–422, 2012.
- [38] Petros Maragos and Ronald Schafer, “Morphological filters–part i: Their set-theoretic analysis and relations to linear shift-invariant filters,” *IEEE Transactions on Acoustics, Speech, and Signal Processing*, vol. 35, no. 8, pp. 1153–1169, 1987.
- [39] Nobuyuki Otsu, “A threshold selection method from gray-level histograms,” *IEEE transactions on systems, man, and cybernetics*, vol. 9, no. 1, pp. 62–66, 1979.
- [40] Ran Yang, Xiang Li, Huan Liu, Yanling Zhen, Xianxiang Zhang, Qiuxia Xiong, Yong Luo, Cailiang Gao, and Wenbing Zeng, “Chest ct severity score: an imaging tool for assessing severe covid-19,” *Radiology: Cardiothoracic Imaging*, vol. 2, no. 2, pp. e200047, 2020.
- [41] Pierre Geurts, Damien Ernst, and Louis Wehenkel, “Extremely randomized trees,” *Machine learning*, vol. 63, pp. 3–42, 2006.